Nonlinear System-identification of the Filling Phase of a Wet-Clutch System

W. D. Widanage[1a], J. Stoev[b], A. Van Mulders[a], J. Schoukens[a], G. Pinte[b]

[a]*Dept. ELEC, Vrije Universiteit Brussel, Pleinlaan 2, B1050 Brussels, Belgium*
[b]*FMTC, Celestijnenlaan 300D, B-3001 Leuven, Belgium*

Abstract

The work presented illustrates how the choice of input perturbation signal and experimental design improves the derived model of a nonlinear system, in particular the dynamics of a wet-clutch system. The relationship between the applied input current signal and resulting output pressure in the filling phase of the clutch is established based on bandlimited periodic signals applied at different current operating points and signals approximating the desired filling current signal. A polynomial nonlinear state space model is estimated and validated over a range of measurements and yields better fits over a linear model, while the performance of either model depends on the perturbation signal used for model estimation.

Keywords: Experiment design, Input signals, Clutches, Nonlinear system, Frequency response, State space

Notation

$u(t)$: Input time signal

P: Number of measured signal periods

[1]Corresponding author. Tel:+32 (0)26292946

fax: +32 (0)26292850

E-mail address: wwidanag@vub.ac.be.

R: Number of independent signal realisations

$U(k)$: Discrete Fourier transform (DFT) of $u(t)$ with k the harmonic number

$U_p^r(k)$: DFT of the *pth* period and of the *rth* realisation of signal $u(t)$

$U^r(k)$: DFT's averaged over periods for a given realisation

$G_p^r(k)$: Frequency response estimated from the *pth* period and of the *rth* realisation of the input and output signal

$G^r(k)$: Frequency response estimate for the *rth* realisation of the input and output signal when averaged over periods

$G(k)$: Final frequency response estimate when averaged over realisations

1. Introduction

The modelling of a system forms a crucial step in engineering practice. Depending on the level of information available at hand the identification procedure is either defined as "white", "grey" or "black" box identification. White box identification is where the system's dynamics are fully known and can be derived from first principles. Grey box identification involves some knowledge of the dynamics which when combined with experimental measurements yields a model and black box identification is when no knowledge regarding the dynamics is known and an arbitrary model is derived by performing experiments (Ljung, 2010). As such the manner in which the experiment is performed, which includes the selection of input excitation and operating regions in which the experiments are carried out, restricts and influences the quality of the final model (Hjalmarsson, 2005). The system modelling and identification method presented here follow a black box approach while an example of modelling using mechanical and friction principles is presented in Nouailletas et al. (2010).

The system to be identified is a wet-clutch device (Figure 1). A wet-clutch is a mechanical device that transmits torque from an input axis to an output axis via fluid friction prior to the engagement of the friction plates. Such devices are commonly used in automatic transmissions for off highway vehicles and agricultural machines to transfer torque from the engine to the load. An electro-hydraulic proportional valve regulates the pressure inside the clutch which causes the engagement of the piston with the friction plates (Figure 2) . A model describing the relation between the current applied to the motor of the elctro-hydraulic valve and the resulting pressure during the filling stage of the clutch is required, to bring about a smooth engagement.

Figure 1: Wet-clutch experimental set-up

With the natural degradation of the wet-clutch over time, an input (control) signal that once resulted in a smooth engagement will not be a suitable signal with time. As such an iterative learning control procedure, whereby at each iteration a control signal similar to the existing signal is applied to find a more appropriate control signal. Such a control scheme as presented in Pinte et al.

(2010) is shown to be an alternative and efficient method over robust control of wet-clutches. It is therefore important to derive a reliable model describing the dynamic behavior around the input signals applied in practise.

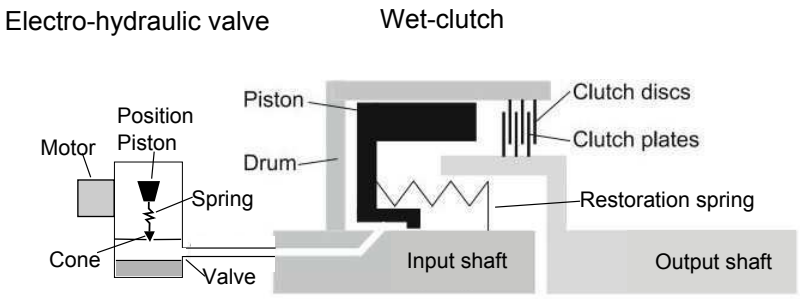

Figure 2: Cross-sectional schematic of the elctro-hydraulic valve and wet-clutch

When engaging the clutch, a fast response without vibrations is expected. Torque transfer should thus commence as soon as possible without introducing torque discontinuities and peaks. This can be realised by a short filling phase followed by a smooth transition into the slip phase (Depraetere et al., 2010).

The model to be derived deals with the filling phase of the clutch. In this region the applied current to the valve and the corresponding clutch pressure can be measured in open loop. This is advantageous for identification as any measurement noise in the output is not present in the measured input or fed through the system. The current signal for model estimation is periodic with its further features and design given in Section 2.2. A linear model in the form of rational finite order transfer function and a polynomial nonlinear state space model relating the current and pressure are estimated and validated. The estimation procedure and comparison of the two models are given in Section 4 of the paper.

2. Experimental Prerequisite

2.1. Wet clutch filling stage

In order to decide the amplitude level (or a signal's root mean square value) and the operating point around which a current signal is expected to be applied, the filling region of the piston needs to be determined. This involves the application of a low current signal to the valve and is gradually increased while observing the corresponding pressure and for any transmission of torque. The piston is initially held back by a restoration spring (Figure 2) and a certain level of oil pressure is required to bring about a displacement. Similarly as the current is increased the pressure in the drum increases pushing the piston towards the friction plates until the transmission of torque is noted. This region is defined as the *filling phase* of the wet clutch. The pressure (Pr) values and the corresponding current (i) applied to the electro-hydraulic value in the filling region are obtained experimentally to be equal to[1]:

$$1.368 \leq Pr \leq 3.3$$

$$0.035 \leq i \leq 0.069$$

The filling region established as mentioned is a steady state region whereby any step change of current in the interval will cause the pressure to rise and settle to a value in the corresponding pressure interval with no transmission of torque. The types of current signals applied within this interval to examine the dynamics are discussed in Section 2.2.1.

Further, by applying a large current pulse that lasts for a short duration the pressure can be increased to values much larger than the steady state interval. A

[1]For reasons of company confidentiality physical units are omitted.

short current pulse width is necessary to ensure that no abrupt torque transmission could occur. As such once the current pulse is applied it is then gradually increased to the point of torque transmission. Such current signals will result in a rapid but smooth engagement and are discussed further in Section 2.2.2.

2.2. Input signal consideration

Periodic perturbation signals offer many advantages over an arbitrary non-periodic excitation when estimating frequency response functions (FRF) and detecting and quantifying non-linear system dynamics (Godfrey, 1993; Pintelon and Schoukens, 2001; Abd-Elrady and Schoukens, 2005). These include the elimination of transient errors from FRF estimates, the reduction of noise effects at the output and detection and quantification of nonlinear distortions. However, careful thought is required during the design of such signals to utilise these advantages. For linear system identification in the presence of noise, signals with high signal to noise ratio over the frequency band of interest are required and if the system is nonlinear, signals with small peak to peak are desired to reduce the effect of nonlinearities present at the output. The generation of additional frequencies in the output signal which are not present in the input signal is an example of a nonlinear phenomenon (Schetzen, 1980). This effect allows the level of the nonlinearity to be detected. By suppressing certain harmonics in the input spectrum, the resulting amplitude levels in the output spectrum at those suppressed harmonics indicates the presence and level of the nonlinear distortions (Evans et al., 1994; D'haene et al., 2005). Further if all even harmonics (including the d.c) are suppressed, the distortions at the even harmonics are due to even order nonlinearities and if some odd harmonics are suppressed, the distortions at the suppressed odd harmonics are due to odd order nonlinearities (Schoukens

et al., 2009).

For these reasons the input signal applied to the electro-hydraulic valve is periodic and bandlimited. Two types of signals are designed for the purpose of estimation, and are:

1. Multisine signals
2. Bandlimited approximation of a filling stage current signal

The design and the choice of such signals are elaborated in the following sections.

2.2.1. Multisine signals

A multisine signal is a sum of sinusoids and offers great design flexibilities both in the spectrum amplitude and harmonic content. The time signal expression is given in equation (1).

$$u(t) = \sum_{k=-M}^{M} U(k) e^{j2\pi k f_s t/N} \tag{1}$$

$$U(k) = A(k) e^{j\phi_k} \tag{2}$$

Such signals allow arbitrary harmonics to be suppressed by setting $U(k) = 0$ while assigning a desired amplitude (power) spectrum in the remaining harmonics. In equation (2) $A(k)$ is the real valued amplitude and ϕ_k is the phase at harmonic k and M denotes the highest harmonic number of the signal. Further, $U(k)$ is a complex variable with $U(-k) = U^*(k)$, f_s is the sampling frequency and N the number of samples per period. For a given amplitude spectrum $A(k)$, the choice of the phase at each harmonic (ϕ_k) will affect the amplitude distribution of the multisine signal $u(t)$ (Schoukens and Dobrowiecki, 1998; Evans et al., 1996). Two amplitude distributions are considered for the estimation of the wet-clutch. In either case the signals have a flat amplitude spectrum and the phases

are selected such that the signal has a normal amplitude distribution or a positively skewed amplitude distribution. The normally distributed signal serves best to investigate the dynamics around an operating point while the skew distributed signal examines how the system responds to a sudden increase in current about a given operating point.

Normally distributed multisine signal

A normal distribution is obtained when the harmonic phase is an independent, identically and uniformly distributed random variable in the interval $[0, 2\pi)$ (Pintelon and Schoukens, 2001). With most of the samples occurring around the signal's mean (or operating point), the signal allows the dynamics around the operating region to be better examined. An example of a such a signal is shown in Figure 3.

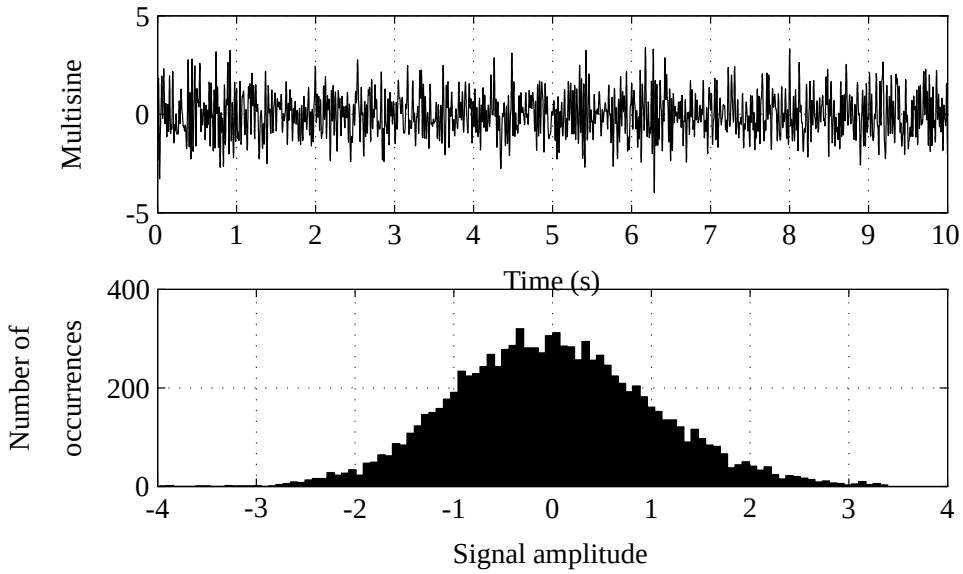

Figure 3: Top figure: Normally distributed multisine signal. Bottom figure: Amplitude distribution

Skew distributed multisine signal

The selection of the harmonic phases for the generation of a positively skewed amplitude distribution involves an iterative process. A brief description of the steps involved is given here with a full description found in Schoukens and Dobrowiecki (1998). Consider a power of a time function of the form $z(t) = at^{\alpha}$, with a a constant positive coefficient and α a constant exponent greater than 1. The rapid increase of the value of $z(t)$ for large values of t implies that the amplitude distribution of $z(t)$ is positively skewed. Based on a normally distributed multisine signal $u_0(t)$, the iterative algorithm arranges the signal $z(t)$ giving a new signal $\tilde{z}(t)$. The phases of the signal $\tilde{z}(t)$ are retained and a new multisine $u_1(t)$ is generated based on these phases and the flat amplitude spectrum. The procedure is repeated by rearranging $z(t)$ now based upon $u_1(t)$ to derive the signal $u_2(t)$, and the iteration ends when a suitable convergence criterion is met. The steps involved are:

1. Generate an initial multisine $u_0(t)$.
2. Generate $z(t)$ with its rms equal to $u_0(t)$.
3. Replace the smallest value of $u_0(t)$ with the smallest value of $z(t)$, followed by the next smallest value of $u_0(t)$ replaced by that of $z(t)$ and so on resulting in $\tilde{z}(t)$.
4. Obtain the phases of $\tilde{z}(t)$ and generate multisine $u_1(t)$ based on these phases and a flat amplitude spectrum.
5. Repeat from Step 3 with $u_1(t)$ instead of $u_0(t)$.

An example of such a signal is shown in Figure 4. Large positive values in the time plot of the signal are observed and the corresponding amplitude distribution shows a positive skewness.

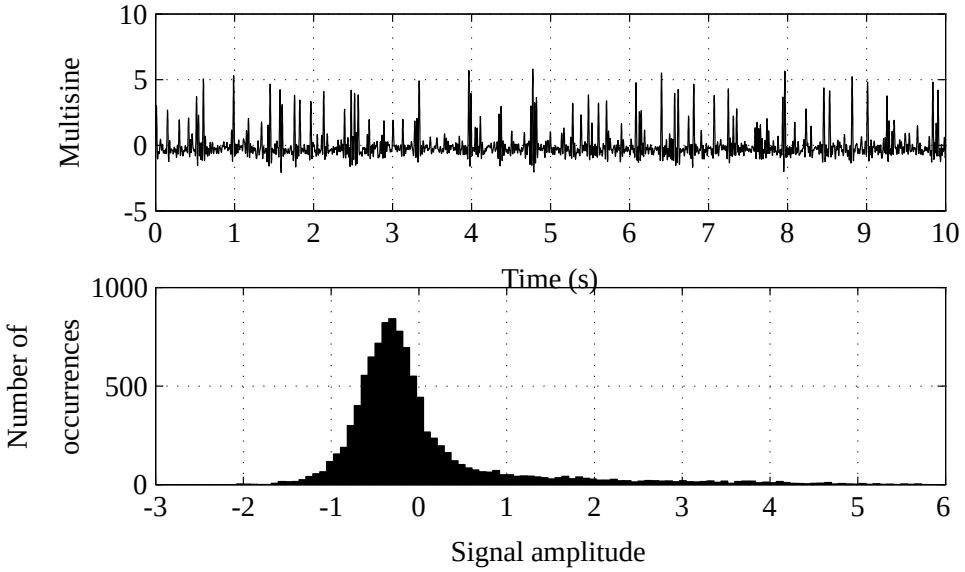

Figure 4: Top figure: Positively skewed multisine signal. Bottom figure: Amplitude distribution

Both the signals shown in Figures 3 and 4 are zero mean signals and have a flat amplitude spectrum from 1-50 Hz.

2.2.2. Bandlimited approximate filling signal

The intended outcome of the filling stage is a smooth engagement of the piston with the friction plates within a short time duration. The sort of current signal that will result in such an engagement is shown in Figure 5.

Starting with some low current value (I_0) the signal has an initial pulse (I_p) applied after a time interval of T_0 and then dropped to value I_3 followed by a gradual increase (ramp) of the current to a final value I_f. The resulting rapid increase in pressure, from the pulse section ensures that the shaft fills with oil quickly forcing the piston closer to the friction plates which is then slowed down and engaged smoothly as a result of the ramp section of the current signal. The total duration of the signal is $T_t = 2.5$s with the pulse lasting for $T_1 = 200$ms.

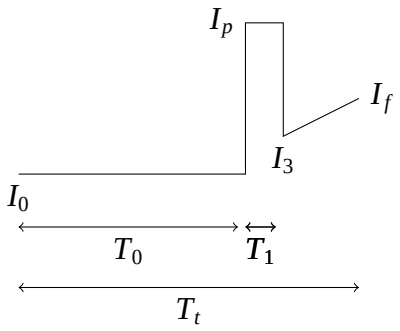

Figure 5: Filling current signal

Having sharp edges, the signal is not bandlimited and consists of all harmonics. As such when used as a perturbation signal there will be more inter harmonic modulation in the output spectrum and results in a poor estimate of the underlying linear dynamics. The discrete Fourier transform (DFT) of a periodic signal $u(t)$ is defined as:

$$U(k) = \frac{1}{\sqrt{N}} \sum_{t=1}^{N} u(t) e^{-2j\pi kt/N}, \quad k = 0, \pm 1, \ldots, \pm M \tag{3}$$

In equation (3) N is the number of samples per period and M the highest harmonic number. By computing the DFT of the desired signal and using the first M harmonics from the transform, a bandlimited signal approximating that of the desired signal (Figure 5) is generated via the inverse discrete Fourier transform (IDFT).

A desired signal and its bandlimited approximation obtained via the truncated DFT method are shown in Figure 6. The approximated signal is a smooth signal and the discrepancy with the desired signal is highest at its discontinuous points (Figure 6). In the example the approximated signal consists of the first 100 harmonics. The desired signal has a signal length of 2.5s giving a fundamental of $1/2.5 = 0.4$Hz. With 100 consecutive harmonics the approximate signal is

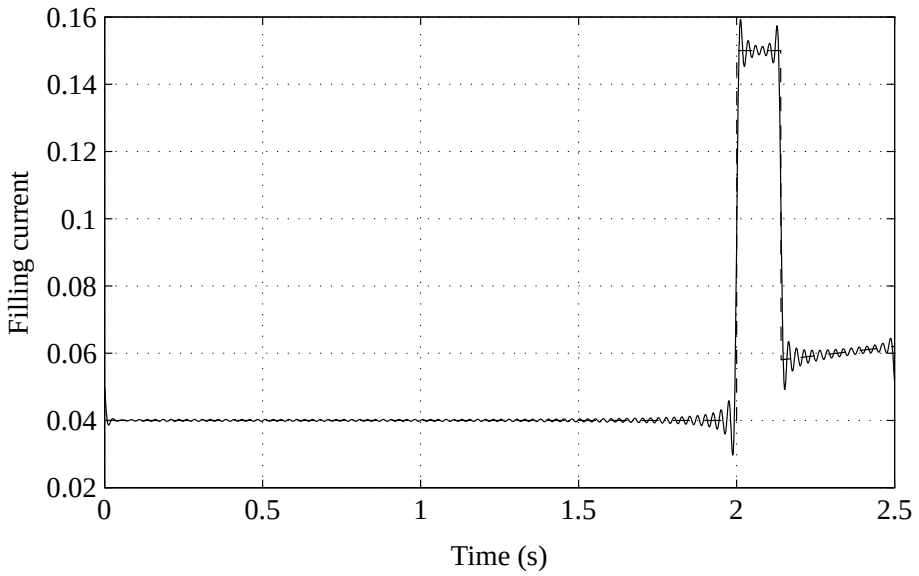

Figure 6: Dash line: Desired filling current. Solid line: Bandlimited approximated version

bandlimited up to 40Hz. The resulting amplitude spectrum (magnitude of the signal's DFT) of the bandlimited signal is shown in Figure 7.

3. Experimental design: Measurements for estimation and validation

3.1. Measurements for model estimation

A linear approximation of a nonlinear system is conditioned by the properties of the input signal. Based on the application, a linear model derived for a given signal's operating point or its standard deviation, can differ when derived for another operating point or standard deviation value (Schoukens et al., 2004). As such for the identification of the wet-clutch model a series of measurements are gathered whereby several input parameters are changed in each measurement experiment. Initially the measurements are carried out by applying a multisine signal at different operating points (mean around which the multisine signal is applied) within the steady state filling interval (Section 2.1). A further set of

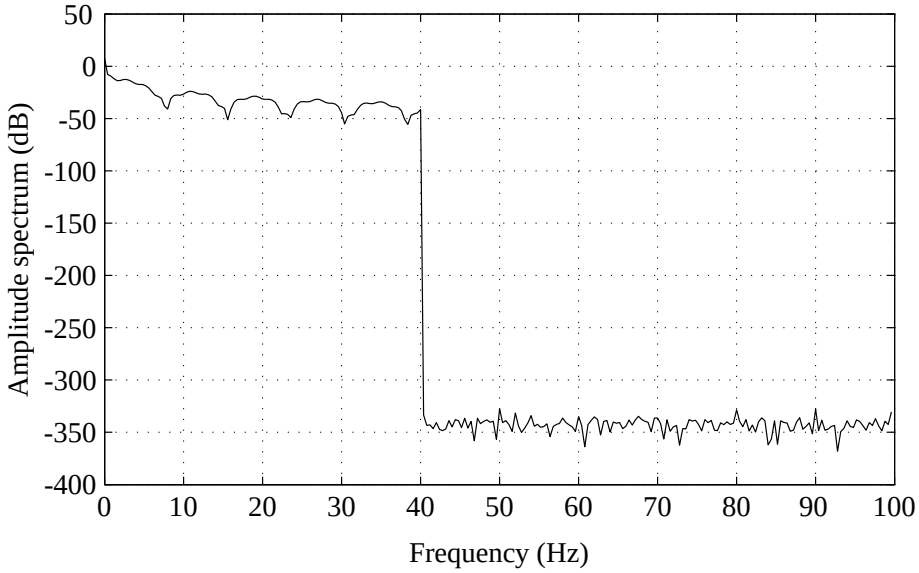

Figure 7: Amplitude spectrum of the bandlimited signal

measurements is obtained by applying the bandlimited approximate current signal coupled with a multisine signal for different values of the signal parameters such as the pulse height, width and final current value (see Figure 5).

From prior experience and preliminary experiments performed on the wet-clutch it was ascertained that a model spanning a low bandwidth will be sufficient to capture the salient features of the system. As such all measurements for model estimation are periodic with a signal period of 10s and is bandlimited up to 50Hz. The applied current signal and corresponding pressure is measured over 100s giving 10 signal periods for averaging and for the analysis of output noise in the measured pressure signal. An estimate of the measurement noise power which is the variance of the measured pressure periods indicates if the data is reliable and also influences the quality of any derived model (D'haene et al., 2005).

The final model is derived based on all the collected measurements and is not confined to a particular measurement set. Since the data are collected by

changing several input parameters and features, the resulting model is expected to be robust and versatile.

3.1.1. Measurements with multisine at several operating points

By applying a multisine current signal at several operating points the variation of the linear dynamics can be examined. For a given operating point the signal standard deviation is adjusted ensuring that the corresponding pressure is within the filling region of the clutch. Table 1 shows 10 operating points at which the multisine current signal is applied along with the signal's standard deviation and the type of amplitude distribution employed.

Realisation	Operating point	Signal standard deviation	Signal distribution
1	0.050	0.030	Positive Skew
2	0.051	0.004	Normal
3	0.052	0.005	Normal
4	0.054	0.006	Normal
5	0.056	0.007	Normal
6	0.057	0.008	Normal
7	0.058	0.009	Normal
8	0.059	0.009	Normal
9	0.060	0.012	Positive Skew
10	0.061	0.015	Positive Skew

Table 1: Selected operating points within the filling stage for model estimation

Figures 3 and 4 presented earlier in Section 2.2 show an example of a single

period of a multisine signal employed for a given operating point. The current signal applied at each operating point is independent and has a new phase realisation (in the case of the normally distributed signal) or a new initial multisine signal $u_0(t)$ (in the case of the case of the skew distributed signal). The harmonic content is however identical and each signal has a bandwidth of 50Hz with several odd and even harmonics suppressed.

3.1.2. Measurements with bandlimited approximate signal

As described in Section 2.2.2, the application of the desired filling signal (Figure 5) is to bring about a smooth engagement of the clutch, and a bandlimited approximate signal is generated for the purpose of identification. Having a signal period of $T_t = 2.5$s, the bandlimited signal is duplicated four times to a give a signal length of 10s making the measurement period consistent with the multisine signals (Section 3.1.1).

Prior to the duplication the bandlimited signal is designed with 100 consecutive harmonics up to 40Hz with a fundamental frequency at 0.4Hz (Figure 7). By repeating the signal four times the new fundamental frequency is now at 0.1Hz (signal length is 10s) and the repetition causes the 100 consecutive harmonics of the original signal to occur at every 4th harmonic relative to the new fundamental frequency of 0.1Hz. As such the signal consists of only even harmonics. The increased frequency resolution is an advantage and is made use of by superimposing a zero mean multisine signal of period length 10s with odd only harmonics up to a frequency range of 50Hz. Due to the linear combination of the two signals (bandlimited approximation and multisine) there is no interharmonic modulation and the amplitude spectrum of the resulting signal shows the distinct frequency content of the individual signals.

While the signal power is mostly from the underlying filling signal the coupling of the multisine is to capture the finer dynamics of the wet clutch since it increases the frequency content if only a bandlimited approximate filling signal were to be used. Figure 8 shows one period of the resulting signal in the time domain. The figure may first appear to present 4 periods of the bandlimited signal repeating every 2.5s (however for instance the pulses are not identical), since the superimposed multisine is 10s in length the final signal is periodic every 10s. The amplitude spectrum shown in Figure 9 shows the contribution from the bandlimited approximate signal (crosses) occurring at even harmonics and the flat spectrum multisine (circles) contribution occurring at the odd harmonics.

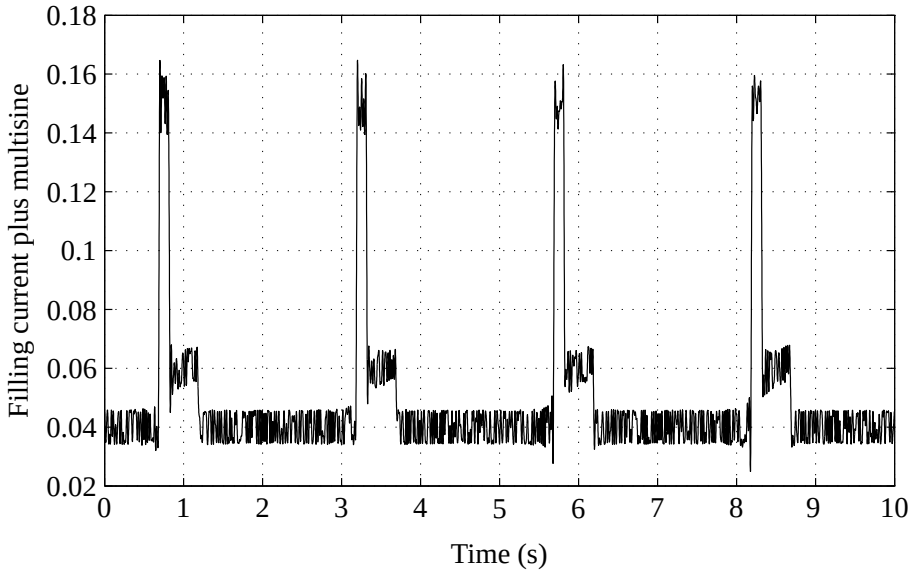

Figure 8: Bandlimited filling signal with a superimposed multisine

Similar to the application of a multisine at different operating points, the wet clutch dynamics are examined for a range of filling current parameter settings. Referring to Figure 5 these include the drop down current I_3, final current I_f, pulse length T_1 and the standard deviation of the superimposed multisine signal.

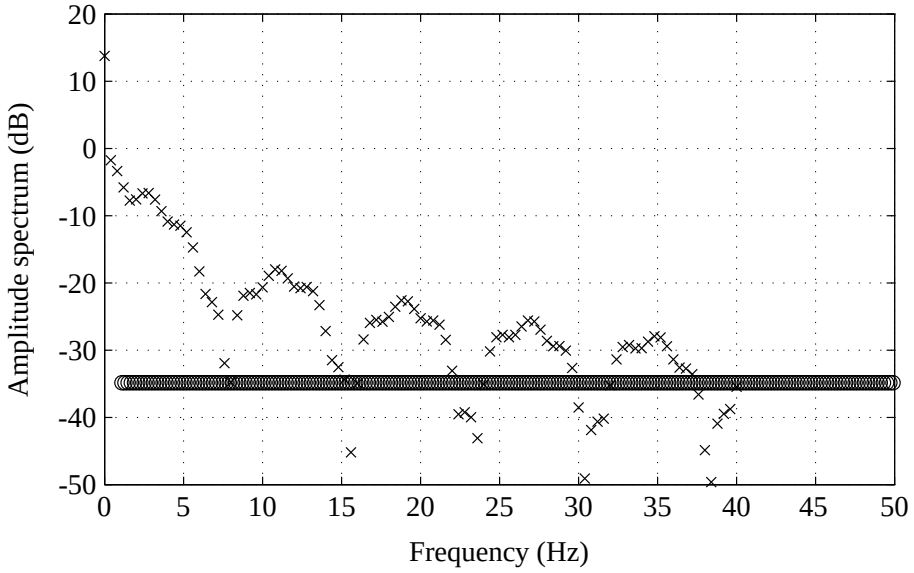

Figure 9: Amplitude spectrum of the filling signal as a combination of two spectra. Crosses: Bandlimited approximate spectrum. Circles: Superimposed multisine spectrum

The selected values of these parameters are shown in Table 2. The remaining parameters of the filling current signal are fixed for each realisation, such as the initial low current $I_0 = 0.04$, pulse height $I_p = 0.15$, the time after which the pulse is applied $T_0 = 2$s.

3.2. Measurements for model validation

Once a model is derived, a new set of input current and output pressure signals are required to validate the model. For this the measurements are carried out with the desired filling current signal that is described in Section 2.2.2. The effectiveness and robustness of the model is examined for a range of parameter settings. In particular 10 measurement sets of input-output data are recorded and Table 3 shows the parameter setting for each of the measurements, while the remaining parameters of the filling current signal are fixed for each realisation, such as the initial low current $I_0 = 0.04$, and the signal length $T_t = 2.5$s. For

Realisation	Drop down current I_3	Final current I_f	Pulse length T_1(ms)	Multisine standard deviation
1	0.058	0.062	130	0.004
2	0.060	0.062	140	0.004
3	0.060	0.060	150	0.004
4	0.058	0.062	160	0.005
5	0.060	0.062	130	0.005
6	0.058	0.062	140	0.005
7	0.058	0.062	150	0.005
8	0.058	0.060	160	0.006
9	0.058	0.062	130	0.006
10	0.058	0.062	140	0.006

Table 2: Parameter settings of the desired filling current signal and multisine signal for model estimation

each realisation 5 periods of the current and corresponding pressure signal are recorded to reduce the influence of measurement noise by signal averaging.

4. Evaluation and analysis of data

4.1. Nonlinear distortion and noise levels

The preliminary data analysis is the investigation of the level of nonlinear distortions and noise. The suppression of several odd and even harmonics in the current multisine signal applied at different operating points (Section 3.1.1) allows the level of nonlinearity to be examined. For a linear system, in the absence of any noise, the output spectrum consists only of the harmonics present

Realisation	Peak current	Drop down current	Final current	Pulse length	Pulse applied after
	I_p	I_3	I_f	T_1(ms)	T_0(s)
1	0.150	0.058	0.062	140	2
2	0.150	0.060	0.062	130	2
3	0.150	0.058	0.060	160	2
4	0.140	0.058	0.062	150	2
5	0.160	0.058	0.062	140	2
6	0.150	0.058	0.064	150	2
7	0.150	0.058	0.062	160	2
8	0.150	0.062	0.062	140	2
9	0.150	0.058	0.062	150	1
10	0.150	0.058	0.064	140	1

Table 3: Parameter settings of the desired filling current signal for model validation

in the input. Therefore by averaging the measured output signal over periods to reduce the effect of noise and observing the power at the harmonics of the output spectrum that do not occur in the input, the level of nonlinear distortions can be gauged.

Denoting $Y_p^r(k)$ as the DFT of the output pressure signal measured as the p^{th} period (of length 10s) of the r^{th} realisation the averaged DFT for a given realisation is:

$$Y^r(k) = \frac{1}{P}\sum_{p=1}^{P} Y_p^r(k) \tag{4}$$

In equation (4) the averaging is performed over periods where $P = 10$ and is

the total number of periods per measurement realisation. An estimate of the variance of $Y^r(k)$ gives the level of measurement noise. Denoting this variance for a particular realisation as $\sigma^{2[r]}(k)$, it is defined as:

$$\sigma^{2[r]}(k) = \frac{1}{(P-1)P} \sum_{p=1}^{P} |Y_p^r(k) - Y^r(k)|^2 \tag{5}$$

In equation (5) the extra division with P is included in order to obtain an estimate of the variance of $Y^r(k)$ instead of $Y_p^r(k)$. This follows from the property that the variance of a sample mean is the variance of the individual samples divided by the total number of samples used in averaging (Papoulis, 1965).

Figure 10 shows the magnitude of $Y^r(k)$ along with nonlinear distortion levels and the noise level ($\sigma^{[r]}(k)$) when the current operating point is at 0.056 and has a standard deviation of 0.007 (measurement realisation 5 in Table 1). The level of even and odd nonlinear distortions are of similar magnitude, with the contributions dominating at the higher frequencies and the noise level is much lower (around -40dB) than the signal amplitude, indicating that the measurements are reliable. Similar conclusions are drawn for the remaining measurements of current applied at different operating points.

4.2. Frequency response function and parametric linear model

For the derivation of a linear model both the measurements of multisines applied at different operating points (described in Section 3.1.1) and measurements with bandlimited approximate signals (described in Section 3.1.2) are used.

Having measured 10 periods and 20 independent realisations the frequency

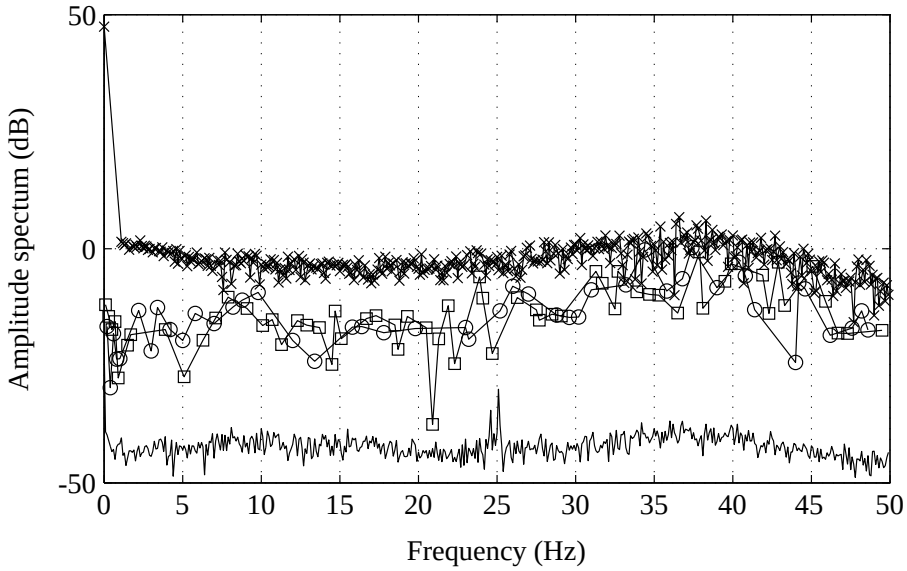

Figure 10: Amplitude spectrum of averaged output signal along with the level of nonlinear distortion and noise. Crosses and line: Amplitude spectrum at harmonics present in the input. Squares and line: Even order distortions. Circles and line: Odd order distortions. Solid line: Measurement noise

response is obtained by subsequent averaging over periods and realisations.

$$G_p^r(k) = \frac{Y_p^r(k)}{U_p^r(k)} \tag{6}$$

$$G^r(k) = \frac{1}{P}\sum_{p=1}^{P} G_p^r(k) \tag{7}$$

$$G(k) = \frac{1}{R}\sum_{r=1}^{R} G^r(k) \tag{8}$$

The term $G^r(k)$ in equation (7) is the individual frequency response obtained for a given realisation, while $G(k)$ in equation (8) is an estimate of the overall frequency response function. In Figure 11 the estimated frequency response magnitude ($|G^r(k)|$) is shown when the wet-clutch is at a low, mid and high operating region of the filling stage, namely measurement realisations 2, 6 and 10

in Table 1. Referring to Figures 11(a), 11(b) and 11(c), it is observed that a change in both gain and resonance frequency occurs depending on the operating point. The overall frequency response $G(k)$ (equation (8)) and an estimate of its standard deviation obtained when all measurements based on different current operating points and bandlimited approximation signals are used, is shown in Figure (12). The standard deviation ($\sigma_G(k)$) is expressed as:

$$\sigma_G^2(k) = \frac{1}{(R-1)R} \sum_{r=1}^{R} |G^r(k) - G(k)|^2 \tag{9}$$

Similar to equation (5) the extra division by R in equation (9) is to estimate the variance of $G(k)$ rather than $G^r(k)$.

Based on the estimated frequency response $G(k)$, a finite order rational transfer function in the z-domain is fitted. Several model orders are fitted among which a single zero three pole model is found to yield a satisfactory fit. The parametric fit of the data is shown in Figure 13 and the pole-zero plot of the transfer function is shown in Figure 14.

4.3. Polynomial nonlinear state space model

The final analysis is the fitting of a nonlinear state space model. In particular the model considered is a polynomial nonlinear state space model (PNLSS) given in equations (10) and (11).

$$\mathbf{x}(t+1) = \mathbf{A}\mathbf{x}(t) + \mathbf{B}u(t) + \mathbf{E}\zeta(t) \tag{10}$$

$$y(t) = \mathbf{C}\mathbf{x}(t) + \mathbf{D}u(t) + \mathbf{F}\eta(t) + e(t) \tag{11}$$

The expressions are in discrete time and ignoring the terms $\mathbf{E}\zeta(t)$ and $\mathbf{F}\eta(t)$ results in a standard linear state space model with $\mathbf{x}(t)$ denoting the states, $y(t)$ the output and $e(t)$ additive noise. The matrices $\mathbf{A} \in \mathbb{R}^{n_a \times n_a}$, $\mathbf{B} \in \mathbb{R}^{n_a \times 1}$, $\mathbf{C} \in \mathbb{R}^{1 \times n_a}$

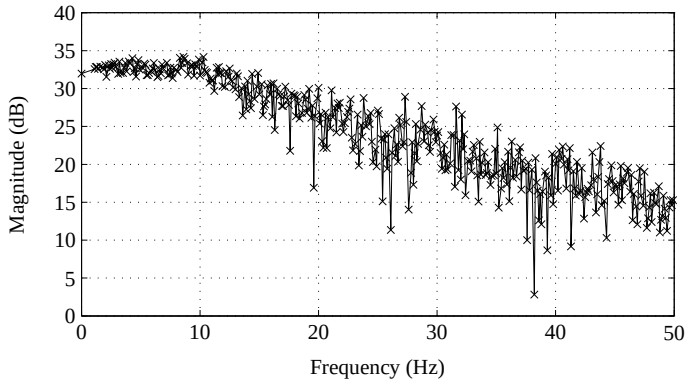

(a)

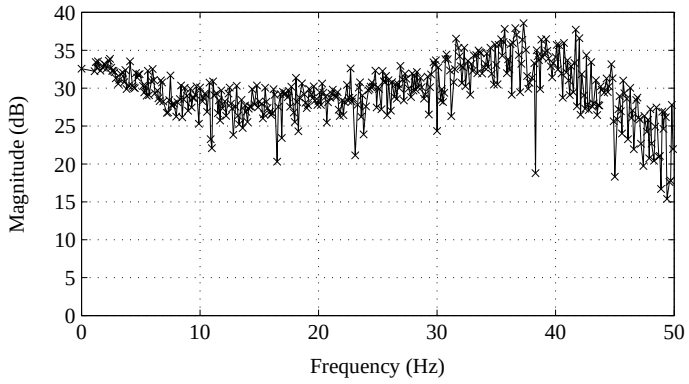

(b)

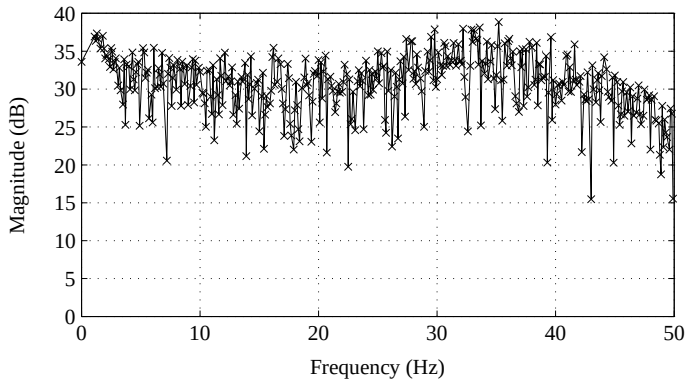

(c)

Figure 11: Variation of frequency response over different operating points in Table 1. (a) Frequency response for realisation 2, operating point: 0.051. (b) Frequency response for realisation 6, operating point: 0.057. (c) Frequency response for realisation 10, operating point: 0.061

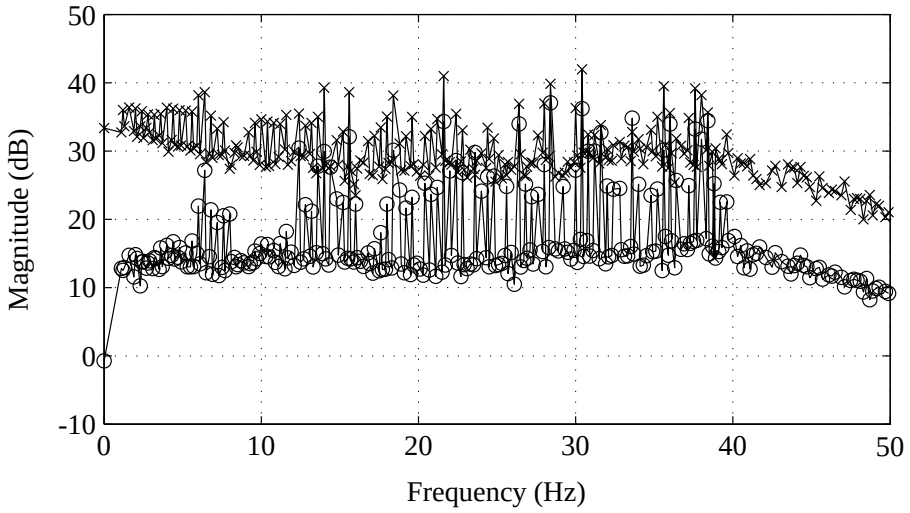

Figure 12: Overall frequency response. Solid line with crosses: Frequency response magnitude. Solid line with circles: Standard deviation

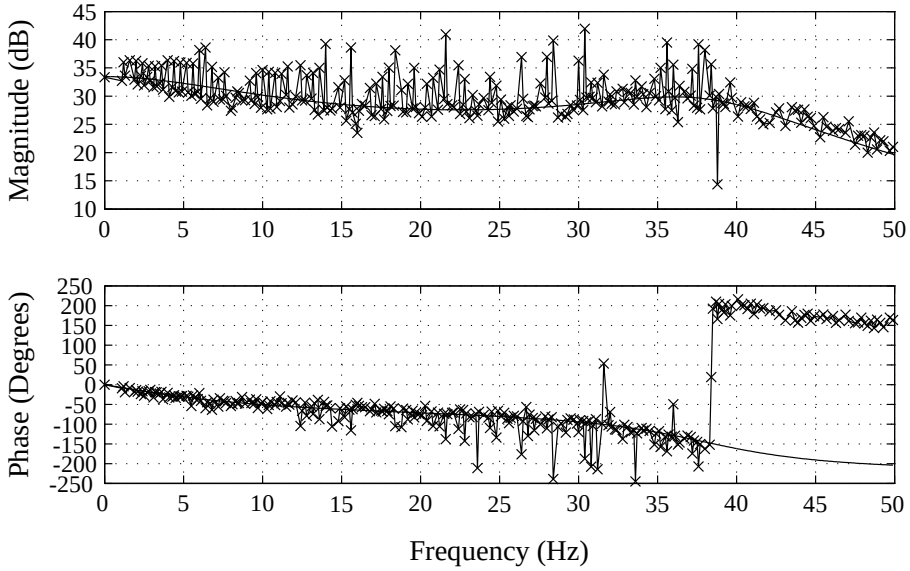

Figure 13: Magnitude and phase of parametric fitting. Top figure, Solid line: Parametric fit magnitude. Solid line with crosses: Estimated frequency response. Bottom figure, Solid line: Parametric fit phase. Solid line with crosses: Estimated phase

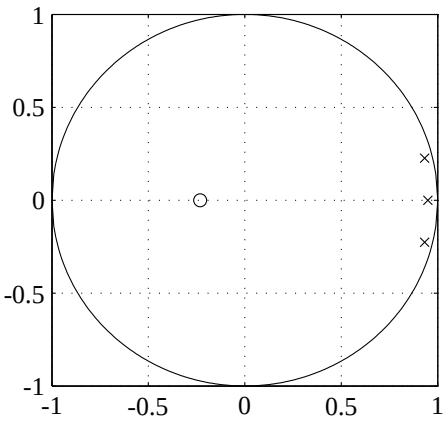

Figure 14: Pole-zero plot and unit circle

and $\mathbf{D} \in \mathbb{R}$ have the coefficients of the linear terms of the states and input. The terms $\zeta(t)$ and $\eta(t)$ are vectors containing monomials of the state and input up to a specified degree with the corresponding coefficients given in matrices $\mathbf{E} \in \mathbb{R}^{n_a \times n_\zeta}$ and $\mathbf{F} \in \mathbb{R}^{1 \times n_\eta}$.

The model shows the separation of the linear dynamics and nonlinear terms. As a nonlinear optimisation routine is required to estimate the matrices in equations (10) and (11), such a structure simplifies the identification procedure. In that, an estimate of the linear model is first derived which can then be used as a starting set of values to estimate the optimum parameter values of the PNLSS model. The steps involved in the estimation of the PNLSS model are as described in Paduart (2007) and Paduart et al. (2010) with the main features of procedure outlined in this section.

From the preceding section a 3rd order (3 pole) linear model is found to give a satisfactory fit on the frequency response data $G(k)$. Therefore a 3 state linear model is identified by minimising the following weighted least squares

cost function (equation (12)).

$$V_{ss} = \sum_{k=1}^{F} |\epsilon(k)|^2 / \sigma_G^2(k) \tag{12}$$

$$\epsilon(k, \mathbf{A}, \mathbf{B}, \mathbf{C}, \mathbf{D}) = G_{ss}(\mathbf{A}, \mathbf{B}, \mathbf{C}, \mathbf{D}, k) - G(k) \tag{13}$$

$$G_{ss}(\mathbf{A}, \mathbf{B}, \mathbf{C}, \mathbf{D}, k) = \mathbf{C}(z_k \mathbf{I}_{n_a} - \mathbf{A})^{-1}\mathbf{B} + \mathbf{D} \tag{14}$$

For this minimisation the starting values for the matrices **A**, **B**, **C** and **D** are obtained through a frequency domain subspace algorithm (Paduart, 2007; McKelvey et al., 1996) and the optimum linear matrices are solved numerically via the Levenberg-Marquardt (LM) algorithm.

The estimation of the PNLSS model involves a further weighted least squares minimisation similar to that of equation (12). The function now minimised is the square error between the output spectrum averaged over periods and that of the PNLSS model.

$$V_{PNLSS}(\theta) = \sum_{k=1}^{F} \|\epsilon(k)\|_2^2 / \|\mathbf{W}(k)\|_2^2 \tag{15}$$

$$\epsilon(k) = [\epsilon^1(k, \theta), \epsilon^2(k, \theta), \ldots, \epsilon^R(k, \theta)]$$

$$\mathbf{W}(k) = [\sigma^{[1]}(k), \sigma^{[2]}(k), \ldots, \sigma^{[R]}(k)]$$

$$\epsilon^r(k, \theta) = Y_m(k, \theta) - Y^r(k) \tag{16}$$

$$\theta = [vec(\mathbf{A})', \mathbf{B}', \mathbf{C}, \mathbf{D}, vec(\mathbf{E})', \mathbf{F}] \tag{17}$$

In equation (15) $\epsilon(k)$ is a vector formed by concatenating the error between the model output and the averaged output spectrum for a given realisation ($Y^r(k)$). Similarly $\mathbf{W}(k)$ is a frequency domain weighting function and is the concatenation of the pressure standard deviation $\sigma^{[r]}(k)$ (equation (5)) estiamted for each realisation. The function $vec(\mathbf{X})$ in equation (17) stacks each column of a matrix **X** to give a column vector. The model output $Y_m(k)$ (equation (16)) is first

calculated in the time domain from the PNLSS model (equation (11)) with the matrices **E** and **F** initially set to zero and matrices **A**, **B**, **C** and **D** set to the optimum values of the linear model obtained from the previous minimisation, after which it is transformed into the frequency domain to calculate the error. Employing the LM algorithm the optimum values of the matrices for the PNLSS model are then solved numerically.

A PNLSS model is first derived using all the 20 estimation realisations (measurements from Tables 1 and 2) consisting of the current signal applied at separate operating points and the approximate filling current signal. A further PNLSS model is then derived based only on the currents applied at different operating points (measurements from Table 1). This analysis intends to establish the importance on the type of estimation data and experiment design when deriving a nonlinear model.

4.4. Validation of linear and nonlinear model

The new set of measured currents and pressure signals with varying current properties as given in Table 3 is used to validate both the PNLSS model and the parametric linear model. Referring to this Table, the data set aims to validate the effectiveness of the derived models for a range of current signal features.

The third order linear parametric model described in Section 4.2 is compared to a three state PNLSS model with the nonlinear monomials in vectors $\zeta(t)$ and $\eta(t)$ (equations (10) and (11)) consisting of state only and input only combinations of up to and including a nonlinear degree of 3. As described in Section 3.2, 5 periods are measured for each of the realisations. The time signals are averaged over the periods and the model output is compared with the averaged pressure signal.

4.4.1. PNLSS and linear model derived using all 20 estimation realisations

The true measured pressure signal (averaged) and the model output of the linear and PNLSS model are shown in Figure 15. The results shown are for the measurements of realisation 3 in Table 3.

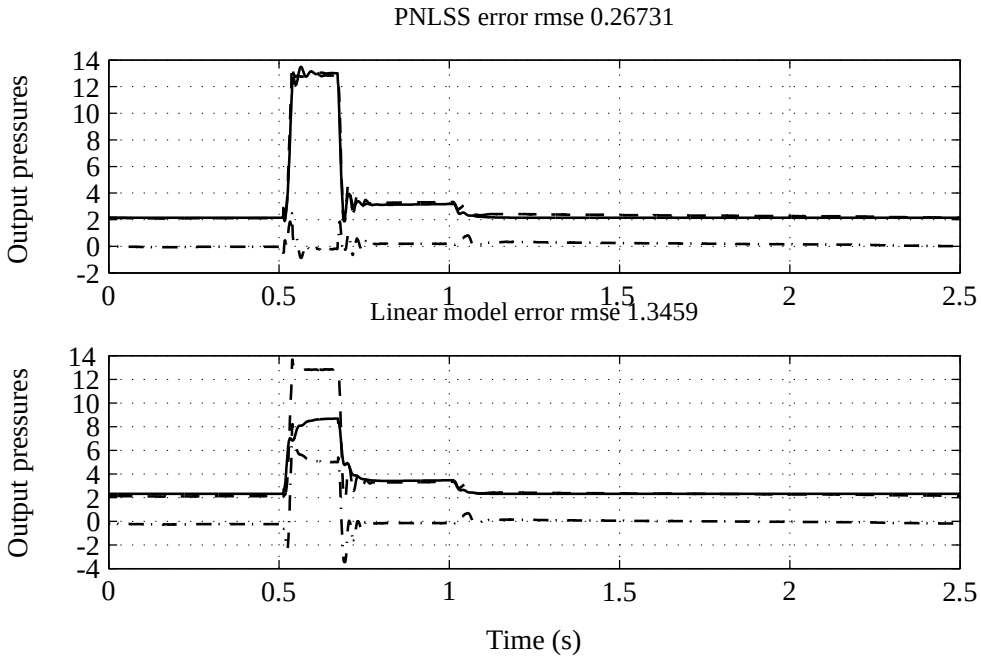

Figure 15: PNLSS and linear model output and error. Top figure, PNLSS model. Bottom figure, Linear model. For both figures, Dash line: Measured pressure. Solid line: Model output. Dash-dot line: Error

For better clarity of the model performance Figure 16 shows the measured and modelled pressure from 0.5s to 1s. When comparing the linear and nonlinear model output the first observation is the vast improvement attained with the PNLSS model with respect to the linear model. It is seen that the gain of the linear model is smaller and the model pressure does not reach the peak pressure of the measured signal. Secondly, with the estimation data consisting of separate operating point measurements and bandlimited approximate filling current

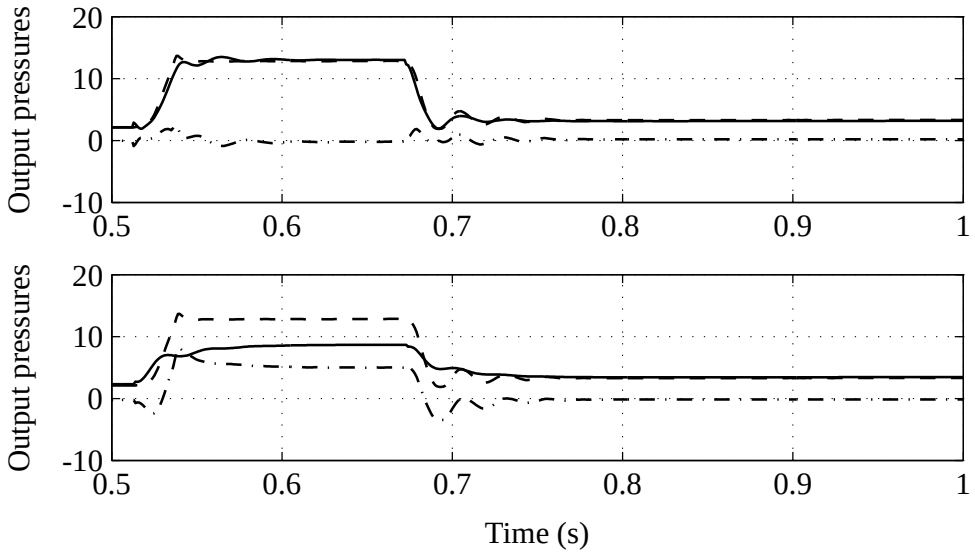

Figure 16: Zoomed time scale of PNLSS and linear model output and error. Top figure, PNLSS model. Bottom figure, Linear model. For both figures, Dash line: Measured pressure. Solid line: Model output. Dash-dot line: Error

signals with multisines added, the PNLSS captures the finer oscillations in the pressure when it rises and falls, while a smooth rise and fall in pressure is observed with the linear model output. Finally the root mean square error (rmse) of the PNLSS model has an improvement by a factor of 5 over the linear model.

The PNLSS model outperforms the linear model for the remaining validation data realisations. This can be observed in Figure 17, where the rmse of both the PNLSS and linear model are plotted against the corresponding validation experiment. It is seen that the PNLSS error level is lower and remains approximately constant with the exceptions of realisations 9 and 10. Here the current signal pulse is applied earlier in contrast to the current signals used in the estimation data. Though the overall model error level increases, the nonlinear model still yields a better fit than the linear model.

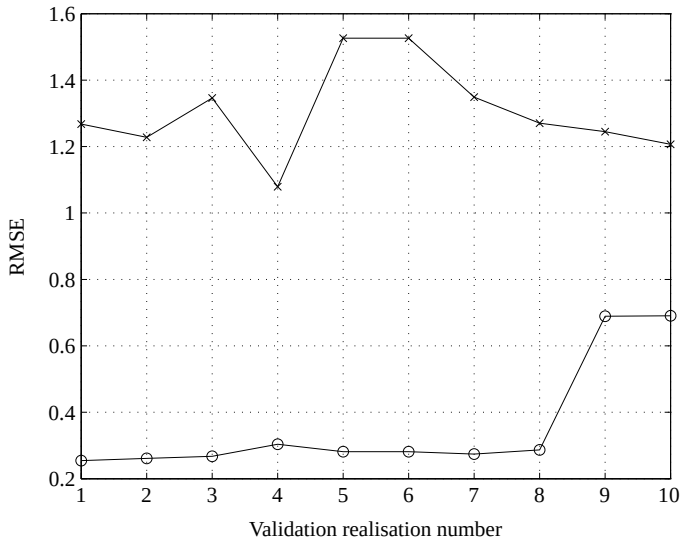

Figure 17: Root mean square error for all the validation realisations. Solid line with crosses: Linear model. Solid line with circles: PNLSS model

4.4.2. PNLSS and linear model derived using only currents applied at different operating points

With the input-output data consisting of the currents applied at the operating points given in Table 1, a 3 pole linear parametric model and a 3 state, 3rd degree nonlinear PNLSS (similar to previous PLNSS model) are estimated. The model outputs when validated with the measurements of realisation 3 in Table 3, are shown in Figure 18. Both models do not fit the peak rise in pressure and the pressure oscillations when rising and falling. However the PNLSS model gives a smaller overall error (rmse) of the two and the conclusion remains true with the remaining validation realisation sets. This can be seen in Figure 19.

The results highlight the importance of the estimation data set when deriving nonlinear models. While the current signals applied at the separate operating points resulted in pressures spanning the filling region of the wet-clutch,

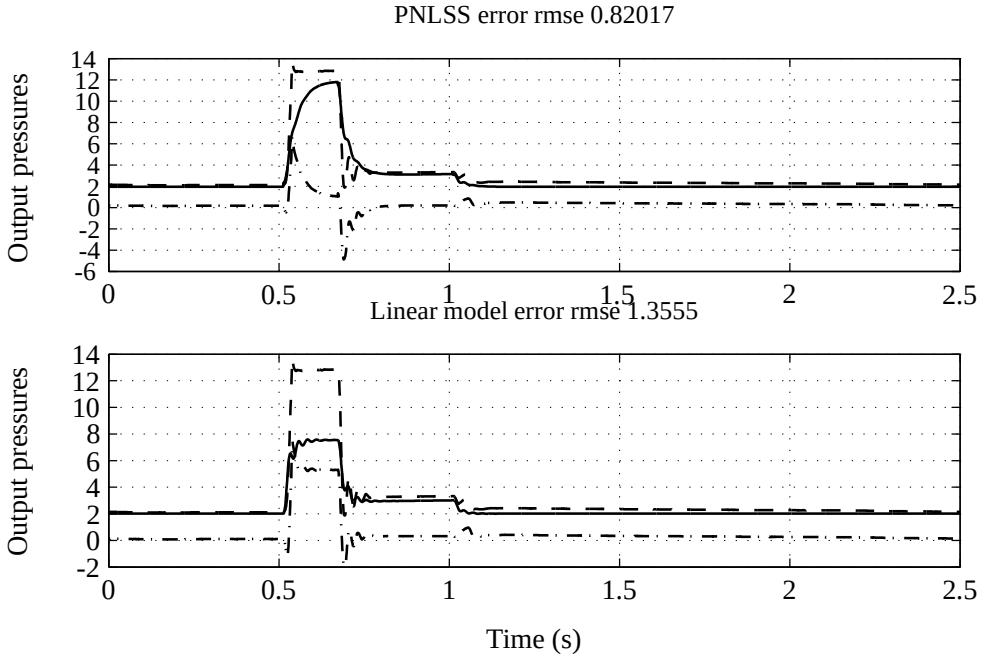

Figure 18: PNLSS and linear model output and error. Top figure, PNLSS model. Bottom figure, Linear model. For both figures, Dash line: Measured pressure. Solid line: Model output. Dash-dot line: Error

the PNLSS model derived based on such measurements does not produce satisfactory fits (Figure 18). However when combined with the approximate filling current data the model output shows a great improvement and the model pressure closely resembles the measured pressure (Figure 15).

5. Conclusions

In comparison to linear system identification careful thought on experimental design with further emphasis on input perturbation signals and their operating points pays off in nonlinear system identification. To this end the use of periodic broadband signals with a finite harmonic content reduces both the influence of measurement noise and the contribution from nonlinear distortions. Using mul-

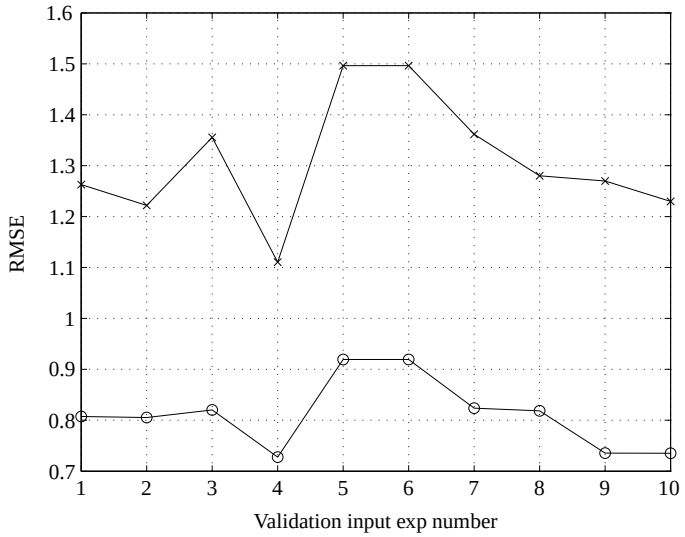

Figure 19: Root mean square error for all the validation realisations. Solid line with crosses: Linear model. Solid line with circles: PNLSS model

tisine signals for model estimation demonstrates its effectiveness in the analysis of the wet-clutch which includes observing the alteration of the linear dynamics (frequency response) and the level of nonlinearity at different operating points.

As bandlimited signals are preferred for model estimation, a bandlimited approximation of a desired signal with an infinite harmonic content can be obtained via the inverse Fourier transform of a finite set of harmonics. This procedure is applied to obtain a current signal that approximates a realistic filling signal.

A polynomial nonlinear state space model of the filling stage of the wet-clutch shows superior results over a linear model for a range of filling current signals. The sources of the better performance are due to the inclusion of the nonlinear terms in the model combined with the diverse set of estimation data, which includes the application of multisines with different amplitude distributions at different operating points and the combination of multisines with bandlimited filling current signals to explore the finer dynamics of the wet clutch

system.

Acknowledgments

The author would like to offer thanks to Bert Stallaert and Bruno Depraetere from Katholieke Universiteit Leuven for their help and ideas. This work was supported in part by the Fund for Scientific Research (FWO - Vlaanderen), by the Flemish Government (Methusalem), by the Belgian Government through the Interuniveristy Poles of Attraction (IAP VI/4) Program and the framework of projects IWT-SBO 80032 of the Institute for the Promotion of Innovation through Science and Technology in Flanders (IWT-Vlaanderen).

References

Abd-Elrady, E., Schoukens, J., (2005). Least-squares periodic signal modelling using orbits of nonlinear odes and fully automated spectral analysis. *Automatica*, 41 (5), 857 – 862.

Depraetere, B., Pinte, G., Swevers, J., (2010). Iterative optimization of the filling phase of wet clutches. *In: Proceedings of the 11th IEEE International Workshop on Advanced Motion Control (AMC 2010)*, 94–9, Nagaoka, Niigata, Japan.

D'haene, T., Pintelon, R., Schoukens, J., Van Gheem, E., (2005). Variance analysis of frequency response function measurements using periodic excitations. *IEEE Transactions on Instrumentation and Measurement*, 54 (4), 1452–1456.

Evans, C., Rees, D., Jones, L., (1994). Non-linear disturbance errors in system identification using multisine test signals. *IEEE Transactions on Instrumentation and Measurement*, 43, 238–244.

Evans, C., Rees, D., Jones, L., Weiss, M., (1996). Periodic signals for measuring non-linear volterra kernels. *IEEE Transactions on Instrumentation and Measurement*, 45, 362–371.

Godfrey, K., (1993). *Perturbation Signals for System Identification*. Prentice Hall.

Hjalmarsson, H., (2005). From experiment design to closed-loop control. *Automatica*, 41 (3), 393 – 438.

Ljung, L., (2010). Perspectives on system identification. *Annual Reviews In Control*, 34 (1), 1–12.

McKelvey, T., Akay, H., Ljung, L., (1996). Subspace-based multivariable system identification from frequency response data. *IEEE Transactions on Automatic Control*, 41(7), 960–979.

Nouailletas, R., Mendes, E., Koenig, D., (2010). Hybrid modeling and identification of dry friction systems, application to a clutch actuator. *Control Engineering Practice*, 18, 904–917.

Paduart, J., (2007). *PhD Thesis: Identification of Nonlinear Systems using Polynomial Nonlinear State Space Models*. VUBPRESS Brussels University Press.

Paduart, J., Lauwers, L., Swevers, J., Smolders, J., Schoukens, J., Pintelon, R., (2010). Identification of systems using polynomial nonlinear state space models. *Automatica*, 46 (4), 647–656.

Papoulis, A., (1965). *Probability, Random Variables and Stochastic Processes*. McGraw-Hill.

Pinte, G., Depraetere, B., Symens, W., Sas, P., Swevers, J., (2010). Iterative learning control for the filling of wet-plate clutches. *Mechanical Systems and Signal Processing*, 24, 1924–1937.

Pintelon, R., Schoukens, J., (2001). *System Identification - A Frequency Domain Approach*. IEEE Press.

Schetzen, M., (1980). *The Volterra and Wiener Theories of Nonlinear Systems*. New York: Wiley.

Schoukens, J., Dobrowiecki, T., (1998). Design of broadband excitation signals with user imposed power spectrum and amplitude distribution. *IEEE Instrumentation and Measurement Technology Conference*, 1002–1005.

Schoukens, J., Lataire, J., Pintelon, R., Vandersteen, G., Dobrowiecki, T., (2009). Robustness issues of the best linear approximation of a nonlinear system. *IEEE Transactions on Instrumentation and Measurement*, 58 (5), 1737–1745.

Schoukens, J., Swevers, J., Pintelon, R., Van der Auweraer, H., (2004). Excitation design for FRF measurements in the presence of non-linear distortions. *Mechanical Systems and Signal Processing*, 18, 727–738.